Ferromagnetic Behavior of Nickel(II)–Imino Nitroxide Derivatives

Dominique Luneau,[1a] Paul Rey,*[,1a] Jean Laugier,[1a] Elie Belorizky,[1b] and André Cogne[1a]

Service d'Etude des Systèmes Moléculaires (UA CNRS 1194), Département de Recherche Fondamentale, Centre d'Etudes Nucléaires, 38041 Grenoble, France, and Laboratoire de Spectrométrie Physique (Associé au CNRS), Université Joseph Fourier, BP87, 38402 Saint-Martin-d'Hères Cedex, France

Received January 2, 1992

Nickel(II) hexafluoroacetylacetonate derivatives of imino nitroxides have been synthesized and structurally characterized. In complex **1**, diaquobis(2-phenyl-4,4,5,5-tetramethyl-4,5-dihydro-1*H*-imidazol-1-oxyl)bis(hexafluoroacetylacetonato)nickel(II), $Ni(hfac)_2(H_2O)_2(IMPh)_2$, the phenyl-substituted free radical is not coordinated to the metal but hydrogen bonded to the aquo metal fragment. On the other hand, in **2**, (2-(2-pyridyl)-4,4,5,5-tetramethyl-4,5-dihydro-1*H*-imidazol-1-oxyl)bis(hexafluoroacetylacetonato)nickel(II), $Ni(hfac)_2IM2\text{-}Py$, and **3**, bis(2,4,4,5,5-pentamethyl-4,5-dihydro-1*H*-imidazol-1-oxyl)bis(hexafluoroacetylacetonato)nickel(II), $Ni(hfac)_2(IMMe)_2$, the 2-pyridyl and methyl-substituted ligands are bound to the Ni(II) ion through the imino nitrogen atom. Magnetic susceptibility measurements show that the metal–radical exchange interaction is ferromagnetic and fairly large (94 and 59 cm^{-1} for **2** and **3**, respectively) in the N-bonded compounds, while the interaction mediated by the hydrogen bond in **1** is weakly antiferromagnetic. These results are rationalized in the frame of the natural magnetic orbital model. Relevant structural data are as follows: **1**, space group $P2_1/n$, a = 11.700 (3) Å, b = 17.928 (4) Å, c = 11.171 (3) Å, β = 107.92 (2)°, Z = 2; **2**, space group $P\bar{1}$, a = 9.277 (3) Å, b = 12.984 (3) Å, c = 13.599 (3) Å, α = 95.03 (1)°, β = 109.17 (1)°, γ = 110.74 (1)°, Z = 2; **3**, space group $P\bar{1}$, a = 10.895 (3) Å, b = 10.934 (3) Å, c = 14.307 (3) Å, α = 82.77 (1)°, β = 84.33 (1)°, γ = 85.77 (1)°, Z = 2.

High-spin molecular-based species[2] may be prepared using two different strategies: (i) one can build clusters of antiferromagnetically coupled spins of different magnitude which do not compensate; (ii) alternatively, one can try to bring into interaction spins residing in orthogonal orbitals. Most of the compounds described so far belong to the first class;[2-7] only a few molecular species in which a high-spin ground state is the result of the orthogonality of the magnetic orbitals have been reported,[2,8-20] and most of them include paramagnetic organic ligands.[9-20] Such a behavior corresponds to special structural arrangements in which the overlap between the magnetic orbitals is not the main cause of the stability of the complexes. Such structural arrangements, bringing two paramagnetic centers in interaction but in which the magnetic orbitals are orthogonal, have been observed for some metal semiquinonates[17,18] and porphyrin cation-radical complexes.[19,20] In these complexes, the metal ion is involved in a planar ring structure; the magnetic orbitals are of σ symmetry on the metal and π symmetry on the radical, and large ferromagnetic interactions have been observed.

In nitroxide magnetochemistry, the sign and the magnitude of the metal–radical coupling constant depend strongly on the nature of both the radical and the metal ion. In O-bonded complexes,[2i,21-24] strongly antiferromagnetic behaviors are the rule except for axial derivatives of copper(II) which exhibit weak ferromagnetic interactions.[9-15] On the other hand, large ferromagnetic couplings have been observed in a few copper(II) adducts[16] of imino nitroxides[25,26] (Figure 1). These organic radicals give N-bonded metal complexes in which a ferromagnetic behavior is related to the binding geometry of the imino nitrogen atom which ensures the orthogonality of the magnetic orbitals.

(1) (a) Centre d'Etudes Nucléaires. (b) Université Joseph Fourier.
(2) For recent reviews, see: (a) Kahn, O. *Angew. Chem., Int. Ed. Engl.* **1985**, *24*, 834–850. (b) Cairns, C. J.; Bush, D. H. *Coord. Chem. Rev.* **1986**, *69*, 1–55. (c) Kahn, O. *Struct. Bonding* **1987**, *68*, 89–167. (d) Miller, J. S.; Epstein, A. J.; Reiff, W. M. *Chem. Rev.* **1988**, *88*, 201–220. (e) Proceedings of the 197th ACS Symposium on Ferromagnetic and High Spin Molecular Based Materials. *Mol. Cryst. Liq. Cryst.* **1989**, *176*. (f) Iwamura, H. *Adv. Phys. Org. Chem.* **1990**, *26*, 179–253. (g) Buchachenko, A. L. *Russ. Chem. Rev. (Engl. Transl.)* **1990**, *59*, 307–319. (h) *Magnetic Molecular Materials*; Gatteschi, D., Kahn, O., Miller, J. S., Palacio, F., Eds.; Nato Asi Series; Kluwer: Dordrecht, The Netherlands 1991; Vol. 198. (i) Caneschi, A.; Gatteschi, D.; Rey, P. *Prog. Inorg. Chem.* **1991**, *39*, 331–431.
(3) Caneschi, A.; Gatteschi, D.; Sessoli, R.; Rey, P. *Acc. Chem. Res.* **1989**, *22*, 392–398.
(4) Pei, Y.; Kahn, O.; Sletten, J. *J. Am. Chem. Soc.* **1986**, *108*, 3143–3145.
(5) Kahn, O.; Pei, Y.; Verdaguer, M.; Renard, J.-P.; Sletten, J. *J. Am. Chem. Soc.* **1988**, *110*, 782–789.
(6) Pei, Y.; Kahn, O.; Nakatani, K.; Codjovi, E.; Mathoniere, C.; Sletten, J. *J. Am. Chem. Soc.* **1991**, *113*, 6558–6564.
(7) Pei, Y.; Journaux, Y.; Kahn, O. *Inorg. Chem.* **1988**, *27*, 399–404.
(8) Kahn, O.; Galy, J.; Journaux, Y.; Jaud, J.; Morgenstern-Badarau, I. *J. Am. Chem. Soc.* **1982**, *104*, 2165–2176.
(9) Anderson, O. P.; Kuechler, T. C. *Inorg. Chem.* **1980**, *19*, 1417–1422.
(10) Bencini, A.; Benelli, C.; Gatteschi, D.; Zanchini, C. *J. Am. Chem. Soc.* **1984**, *106*, 5813–5817.
(11) Grand, A.; Rey, P.; Subra, R. *Inorg. Chem.* **1983**, *22*, 391–394.
(12) Caneschi, A.; Gatteschi, D.; Laugier, J.; Rey, P. *J. Am. Chem. Soc.* **1987**, *109*, 2191–2192.
(13) Caneschi, A.; Gatteschi, D.; Grand, A.; Laugier, J.; Pardi, L.; Rey, P. *Inorg. Chem.* **1988**, *27*, 1031–1035.
(14) Ovcharenko, V. I.; Ikorski, V. N.; Podberezskaya, N. V.; Pervukhina, N. V.; Larionov, S. V. *Russ. J. Inorg. Chem. (Engl. Transl.)* **1987**, *32*, 844–846.
(15) Burdukov, A. B.; Ovcharenko, V. I.; Ikorski, V. N.; Pervukhina, N. V.; Podberezskaya, N. V.; Grigor'ev, I. A.; Larionov, S. V.; Volodarski, L. B. *Inorg. Chem.* **1991**, *30*, 972–976.
(16) Luneau, D.; Rey, P.; Laugier, J.; Friess, P.; Caneschi, A.; Gatteschi, D.; Sessoli, R. *J. Am. Chem. Soc.* **1991**, *113*, 1245–1241.
(17) Kahn, O.; Prins, R.; Reedijk, J.; Thompson, J. S. *Inorg. Chem.* **1987**, *26*, 3557–3561.
(18) Benelli, C.; Dei, A.; Gatteschi, D.; Pardi, L. *Inorg. Chem.* **1988**, *27*, 2831–2836.
(19) Erler, B. S.; Scholz, W. F.; Lee, Y. J.; Scheidt, W. R.; Reed, C. A. *J. Am. Chem. Soc.* **1987**, *109*, 2644–2652.
(20) Gans, P.; Buisson, G.; Duée, E.; Marchon, J.-C.; Erler, B. S.; Scholz, W. F.; Reed, C. A. *J. Am. Chem. Soc.* **1986**, *108*, 1223–1234.
(21) Lim, Y. Y.; Drago, R. S. *Inorg. Chem.* **1972**, *11*, 1334–1338.
(22) Dickman, M. H.; Doedens, R. J. *Inorg. Chem.* **1981**, *20*, 2677–2681.
(23) Porter, L. C.; Dickman, M. H.; Doedens, R. J. *Inorg. Chem.* **1986**, *25*, 678–684.
(24) Porter, L. C.; Dickman, M. H.; Doedens, R. J. *Inorg. Chem.* **1988**, *27*, 1548–1552.
(25) Ullman, E. F.; Osiecki, J. H.; Boocock, D. G. B.; Darcy, R. *J. Am. Chem. Soc.* **1972**, *94*, 7049–7059.
(26) Ullman, E. F.; Call, L.; Osiecki, J. H. *J. Org. Chem.* **1970**, *35*, 3623–3631.

0020-1669/92/1331-3578$03.00/0

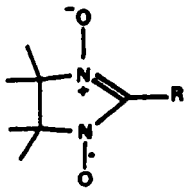

R = Ph, NITPh

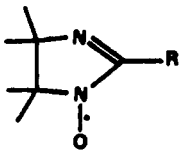

R = Me, IMMe

R = Ph, IMPh

R = 2-Py, IM2-Py

Figure 1. Chemical structure of the nitronyl and imino nitroxides.

Table I. Crystallographic Data and Experimental Parameters[a]

	1	2	3
chem formula	$C_{36}H_{40}F_{12}N_4O_8Ni$	$C_{22}H_{18}F_{12}N_3O_5Ni$	$C_{26}H_{32}F_{12}N_4O_6Ni$
fw	943.4	691.1	783.2
space group	$P2_1/n$	$P\bar{1}$	$P\bar{1}$
a, Å	11.700 (3)	9.277 (3)	10.895 (3)
b, Å	17.928 (4)	12.984 (3)	10.934 (3)
c, Å	11.171 (3)	13.599 (3)	14.307 (3)
α, deg		95.03 (1)	82.77 (1)
β, deg	107.92 (1)	109.17 (1)	84.33 (1)
γ, deg		110.74 (1)	85.77 (1)
V, Å^3	2229.3	1407.3	1679.3
Z	2	2	2
T, °C	20	20	20
ρ_{calcd}, g cm^{-3}	1.406	1.631	1.554
μ, cm^{-1}	5.64	8.76	6.8
R^b	0.056	0.064	0.043
R^c	0.063	0.069	0.041

[a] A summary of experimental data is found in Table SI, deposited as supplementary material. [b] $(\Sigma|F_o - F_c|/\Sigma F_o$. [c] $(\sum w(F_o - F_o)^2/\sum wF_o^2)^{1/2}$.

Assuming that these binding properties hold for all first row transition metal ions, one expects ferromagnetic interactions in octahedral nickel(II) derivatives because the two magnetic orbitals have respectively the same symmetry as that of copper(II) in the reported examples. We describe hereunder such a study of (imino nitroxide)nickel(II) adducts which shows that, indeed, fairly large metal–nitroxide ferromagnetic interactions are also observed in this case. Comparison of the properties of three examples affords information about the coordination chemistry of these free-radical ligands and brings basic information for understanding magneto–structural correlations in the related complexes.

Experimental Section

Syntheses. The imino nitroxides IMPh, IM2-Py, and IMMe (see Figure 1) were prepared according to reported procedures.[25,26]

Diaquobis(2-phenyl-4,4,5,5-tetramethyl-4,5-dihydro-1*H*-imidazol-1-oxyl)bis(hexafluoroacetylacetonato)nickel(II), Ni(hfac)$_2$(H$_2$O)$_2$(IMPh)$_2$ (1). In 5 mL of diethyl ether were dissolved 250 mg of Ni(hfac)$_2$·2H$_2$O and 234 mg of IMPh. To the red brown solution was added 5 mL of heptane, and the diethyl ether was evaporated off by warming with stirring. Large parallelepipedic brown crystals formed after standing 12 h at 4 °C (204 mg, 42%, mp 176 °C). Anal. Calcd for $C_{36}H_{40}F_{12}N_4O_8Ni$: C, 45.81; H, 4.27; F, 24.17; N, 5.94; O, 13.57; Ni, 6.22. Found: C, 45.86; H, 4.08; F, 24.54; N, 5.98; Ni, 6.21.

(2-(2-Pyridyl)-4,4,5,5-tetramethyl-4,5-dihydro-1*H*-imidazol-1-oxyl)-bis(hexafluoroacetylacetonato)nickel(II), Ni(hfac)$_2$IM2-Py (2). This complex was prepared by the same procedure except that the diethyl ether–heptane solution was allowed to evaporate in the dark at room temperature. Thus, 117 mg of IM2-Py afforded 212 mg (58%, mp 166 °C) of the complex as dark-brown crystals. Anal. Calcd for $C_{22}H_{18}F_{12}N_3O_5Ni$: C, 38.23; H, 2.62; F, 32.99; N, 6.08; Ni, 8.50. Found: C, 38.25; H, 2.40; N, 6.27; F, 32.87; Ni, 8.41.

Bis(2,4,4,5,5-pentamethyl-4,5-dihydro-1*H*-imidazol-1-oxyl)bis-(hexafluoroacetylacetonato)nickel(II), Ni(hfac)$_2$(IMMe)$_2$ (3). A diethyl ether–heptane (1/1, 10 mL) solution obtained from 187 mg of Ni(hfac)$_2$·2H$_2$O and 114 mg of IMMe was allowed to stand 1 night at 4 °C. Large brown crystals were obtained (223 mg, 77%, mp 187 °C) which analyzed satisfactorily for $C_{26}H_{32}F_{12}N_4O_6Ni$. Anal. Calcd: C, 39.85; H, 4.12; F, 29.12; N, 7.16; O, 12.26; Ni, 7.50. Found: C, 39.65; H, 4.01; F, 28.72; N, 7.01; Ni, 7.63.

In all cases the crystals were suitable for X-ray diffraction experiments.

Magnetic Measurements. Magnetic data have been collected using a Quantum Design MPMS superconducting SQUID susceptometer working at a 0.5-T field strength in the 2–300 K temperature range. The SQUID outputs were corrected for the contribution of the sample holder, and the magnetic susceptibilities, for the diamagnetism of the constituant atoms by use of the Pascal constants.

X-ray Data Collection and Structure Determination. Weissenberg photographs showed the monoclinic system for **1** and the triclinic system for **2** and **3**. Crystals of approximate dimensions 0.2 × 0.2 × 0.2 mm were mounted on an Enraf-Nonius four-circle diffractometer equipped with graphite-monochromatized Mo Kα radiation. The unit cell parameters were obtained by a least-squares fit of the automatically centered settings from 25 reflections; they are reported in Table I with pertinent details regarding the determination of all three structures. Intensity data were corrected for Lorentz and polarization effects but not for absorption.

Concerning **1**, the $P2_1/n$ space group was established from systematic absences, while the initial choice of the centrosymmetric space group $P\bar{1}$ for the two other compounds was fully confirmed by all subsequent developments during the structure determinations. The structures of **1** and **3** were solved by standard heavy-atom methods using the SHELX76 package.[27] Difference Fourier maps revealed electron density contributions appropriately located for all non-hydrogen atoms. These were refined anisotropically; in the last refinement model, hydrogen atoms were included in fixed and calculated positions with isotropic thermal parameters equal to those of the connected carbon atoms. In the case of **2**, it was noted that the cell parameters were, within a few percent, identical to those of the previously reported structure of Cu(hfac)$_2$IM2-Py.[16] Therefore, it was assumed that the two molecular structures had strong similarities and the positional parameters of the copper derivative were used as a refinement model. In converging to $R = 0.064$, the refinement confirms the pertinency of the assumption that the two molecular structures were strongly related. Atomic positional parameters are listed in Tables II–IV for **1–3**, respectively; selected bond lengths and angles are found in Table V. A summary of crystal data and experimental parameters (Table SI), complete listings of bond lengths (Tables SII–SIV) and angles (Tables SVI–SVII), and listings of anisotropic thermal parameters (Tables SVIII–SX) are deposited as supplementary material.

Results

Structural Studies. Compound **1** (Figure 2) is a centrosymmetric bis(nitroxide) compound where both the imino and nitroxyl groups of the radical *are not bound* to the metal. The metal ion is surrounded by six oxygen atoms, four belonging to the hexafluorinated ligands and the two others to water molecules; as shown in Table V, the metal environment is close to octahedral. The structural characteristics of the free radical moiety are unexceptional and similar to those previously described for imino nitroxides in other metal complexes.[16,28] The O3–N1–C6–N2 fragment is planar, and the angle between this plane and the phenyl ring is 32°. Hydrogen bonding between the aquo ligand and the nitroxide imino nitrogen occurs with the usual structural parameters[29] (N2–Hw1 = 1.70 (6) Å, Ow–Hw1–N2 = 175 (7)°). In the crystal, no intermolecular contact shorter than 5 Å between uncoordinated NO groups nor stacking of phenyl groups belonging to neighboring molecules was observed.

As stated in the Experimental Section, compound **2** (Figure 3) is quasi isomorphous to the copper analogue[16] except for slightly longer equatorial and shorter axial bonds as expected for Ni(II) derivatives. Although the bonding distances are all close to 2.050 Å, significant deviations from an idealized octahedral bonding pattern show up in the bond angles. The main distortion arises in the chelate ring, where the N1–Ni–N3 angle is 78.9 (2)°.

(27) Sheldrick, G. SHELX76 *System of Computing Programs*. University of Cambridge, Cambridge, England, 1976.
(28) Cogne, A.; Grand, A.; Rey, P.; Subra, A. *J. Am. Chem. Soc.* **1989**, *111*, 3230–3238.
(29) Pauling, L. *The Nature of the Chemical Bond*; Cornell University Press: Ithaca, NY, 1976; p 449.

Table II. Positional Parameters (×10⁴) and B Values (Å²) for Ni(hfac)₂(H₂O)₂(IMPh)₂ (**1**)

	x	y	z	B^a
Ni	0 (0)	0 (0)	0 (0)	3.19
O1	893 (2)	−321 (2)	1773 (2)	4.05
O2	−1469 (2)	260 (2)	505 (2)	4.26
OW	641 (3)	1064 (2)	341 (3)	4.69
Hw1	1374 (61)	1234 (38)	1140 (69)	11.39
Hw2	213 (46)	1388 (29)	171 (49)	5.67
C1	415 (4)	−372 (2)	2616 (4)	4.35
C2	1258 (5)	−686 (4)	3854 (5)	7.17
C3	−731 (4)	−193 (3)	2603 (4)	5.13
C4	−1573 (3)	125 (2)	1549 (4)	4.23
C5	−2786 (4)	338 (3)	1677 (5)	6.07
F1	1896 (5)	−126 (3)	4514 (4)	13.74
F2	2038 (4)	−1131 (3)	3696 (4)	13.67
F3	751 (4)	−949 (3)	4616 (4)	11.97
F4	−2974 (3)	112 (3)	2712 (3)	12.05
F5	−3685 (2)	74 (2)	774 (3)	8.34
F6	−2948 (3)	1054 (2)	1602 (5)	14.56
O3	3815 (3)	2880 (2)	4614 (3)	7.47
N1	3577 (3)	2355 (2)	3816 (3)	4.99
N2	2446 (3)	1551 (2)	2447 (3)	4.94
C6	2428 (3)	2119 (2)	3137 (4)	4.00
C7	4479 (4)	1817 (3)	3643 (6)	7.32
C8	3703 (4)	1354 (3)	2561 (5)	6.09
C9	3857 (5)	543 (4)	2559 (9)	11.23
C10	3879 (6)	1621 (6)	1308 (7)	11.62
C11	5599 (6)	2135 (5)	3674 (11)	17.69
C12	4769 (8)	1312 (6)	4908 (7)	13.30
C13	1341 (3)	2494 (2)	3201 (4)	4.49
C14	298 (4)	2062 (3)	2998 (5)	6.98
C15	−760 (4)	2408 (3)	2989 (7)	9.47
C16	−794 (5)	3154 (3)	3192 (6)	8.58
C17	211 (5)	3577 (3)	3395 (6)	7.69
C18	1293 (4)	3257 (3)	3409 (5)	5.91

^{a} Defined as $(4/3)a^2B(1,1) + b^2B(2,2) + c^2(B(3,3) + ab(\cos\gamma)B(1,2) + ac(\cos\beta)B(1,3) + bc(\cos\alpha)B(2,3)$.

Table III. Positional Parameters (×10⁴) and B Values (Å²) for Ni(hfac)₂IM2-Py (**2**)

	x	y	z	B^a
Ni	−66 (1)	2058 (1)	2284 (1)	3.83
O1	−2191 (5)	1371 (3)	2583 (3)	4.57
O2	−1477 (5)	2089 (4)	787 (3)	4.81
O3	−34 (6)	3569 (4)	2828 (4)	5.44
O4	1984 (5)	2911 (3)	1953 (3)	4.62
O5	2638 (8)	−217 (5)	4603 (5)	8.76
N1	1363 (6)	1816 (4)	3679 (4)	3.89
N2	2366 (7)	672 (5)	4505 (4)	5.43
N3	−228 (6)	454 (4)	1773 (4)	3.71
C1	−3493 (9)	1479 (6)	2063 (6)	5.31
C2	−3962 (9)	1795 (6)	1085 (6)	5.51
C3	−2898 (9)	2060 (6)	547 (5)	5.05
C4	−3594 (19)	2362 (15)	−478 (12)	11.32
C5	−4728 (12)	1211 (9)	2610 (10)	8.21
C6	2493 (8)	3922 (5)	1920 (6)	4.83
C7	1941 (9)	4746 (6)	2222 (6)	5.56
C8	713 (9)	4472 (6)	2628 (6)	5.63
C9	179 (15)	5426 (8)	2894 (12)	9.74
C10	3947 (12)	4352 (7)	1610 (9)	7.77
C11	1466 (7)	859 (5)	3580 (5)	3.99
C12	2316 (9)	2468 (6)	4821 (5)	5.21
C13	3030 (8)	1653 (6)	5403 (5)	5.09
C14	4938 (9)	2082 (7)	5867 (8)	8.57
C15	2316 (12)	1221 (8)	6227 (7)	8.65
C16	3661 (12)	3559 (6)	4806 (7)	9.09
C17	1069 (14)	2694 (10)	5202 (7)	10.02
C18	606 (7)	37 (5)	2537 (5)	3.77
C19	600 (8)	−1019 (5)	2345 (6)	5.14
C20	−279 (9)	−1681 (6)	1303 (7)	6.34
C21	−1151 (9)	−1262 (6)	513 (6)	5.85
C22	−1071 (8)	−191 (5)	787 (5)	4.74
F1	−2633 (14)	3288 (12)	−561 (11)	23.64
F2	−3444 (24)	1849 (19)	−1235 (7)	22.86
F3	−4952 (10)	2370 (11)	−811 (7)	17.49
F4	−4810 (8)	472 (7)	3102 (7)	13.92
F5	−6204 (8)	1124 (8)	2012 (7)	13.81
F6	−4288 (16)	2120 (10)	3351 (10)	24.68
F7	−1267 (8)	5157 (5)	2658 (11)	23.22
F8	945 (9)	6372 (5)	2730 (8)	15.15
F9	769 (18)	5745 (9)	3950 (9)	22.19
F10	4834 (7)	5401 (4)	1859 (5)	11.13
F11	4909 (12)	3887 (9)	1871 (14)	25.27
F12	3496 (13)	4101 (9)	597 (8)	24.01

^{a} Defined as $(4/3)a^2B(1,1) + b^2B(2,2) + c^2B(3,3) + ab(\cos\gamma)B(1,2) + ac(\cos\beta)B(1,3) + bc(\cos\alpha)B(2,3)$.

Features similar to those found in the copper analogue are observed; of special interest is the almost perfect planarity of all the atoms of the nitroxide (except the methyl groups) and the metal ion. Similarities are also found in the intermolecular arrangement, which shows a fairly short contact (3.97 (1) Å) between uncoordinated NO groups related by an inversion center which must be taken into account when considering the magnetic properties.

The third complex, **3** (Figure 4), also is a centrosymmetric bis(nitroxide) adduct. The triclinic cell comprises two different molecules. Close inspection of Table V shows that these molecules are very similar: for example, differences of less than 0.01 Å in binding distances and of less than 1° in angles are observed within the metal coordination spheres. Moreover, the binding geometry of the radical is identical in both molecules with the metal ion included in the π plane (N1C6N2O3 and N3C19N4O6) of the nitroxide, which is almost perpendicular (81° in A and 79° in B) to the hexafluoroacetylacetonato mean plane. Thus, in both cases, the π^* direction of the nitroxide is parallel to the metal basal plane and perpendicular to the Ni–N direction (84 (1)° in A and 89 (1)° in B). Noteworthy is the elongated octahedral environment of the nickel in both cases in contrast to that found in **1** and **2**; the imino nitroxides are axially bound (Ni1–N1 = 2.202 (3) Å, Ni2–N3 = 2.172 (3) Å). Finally, the relative orientation of the two molecules is such that their main axes (O3–O'3 and O6–O'6) are almost perpendicular (93.6°) and several short intermolecular contacts (3.57 (1), 3.78 (1) Å) between uncoordinated NO groups related by cell translations are observed.

Magnetic Studies. Magnetic data are shown in Figures 5–7 for **1**–**3**, respectively, in the form of χT vs T. In **1**, the χT product is nearly constant down to 30 K and then decreases sharply on lowering the temperature. The room-temperature value (1.96 emu·K, μ_{eff} = 3.96 μ_B) is close to that expected for independent spins. Indeed, in the same range of temperature, Ni(hfac)₂·2H₂O exhibits Curie behavior down to 3 K with a Curie constant of 1.23 emu·K. Therefore, assuming g = 2 for the organic free radicals, one ends up with χT = 1.98 emu·K for the room-temperature value of the complex assuming uncoupled spins. Interestingly, the behavior of the metal fragment also shows that, in the studied temperature range, a zero field splitting associated with the nickel ion is not operative. Owing to the almost perfect octahedral environment of the metal ion and remembering that large intermolecular distances are observed in the structure, the magnetic data were interpreted[30] considering only an isolated three-spin system involving a Ni(II) ion in cubic symmetry. During the fitting process, it was noticed that the nitroxide–metal interaction and the agreement factor value were nearly independent of the nitroxide–nitroxide exchange parameter. Accordingly, the latter was set to zero. The agreement between observed and calculated data using this model is indeed good, and the values of the parameters are reported in Table VI.

The magnetic behavior of compound **2** is closely related to that of **1** except that on lowering the temperature the χT product first increases from 1.99 emu·K (3.99 μ_B) at room temperature to 2.13 emu·K (4.13 μ_B) at 25 K and then decreases to 1.6 emu·K (3.05 μ_B) at 2 K. In contrast to **1**, the room-temperature value is higher than that expected for independent spins (=1.6 emu·K, 3.6 μ_B)

(30) Sinn, E. *Coord. Chem. Rev.* **1970**, *5*, 313–347.

Table IV. Positional Parameters ($\times 10^4$) and B Values (Å^2) for Ni(hfac)$_2$(IMMe)$_2$ (3)

	x	y	z	B[a]
Ni1	0 (0)	0 (0)	0 (0)	3.69
O1	1620 (2)	722 (2)	134 (2)	4.19
O2	−205 (2)	−419 (2)	1426 (2)	4.25
O3	1242 (3)	−4944 (3)	721 (3)	7.75
N1	884 (3)	−1864 (3)	−85 (2)	3.88
N2	1360 (3)	−3868 (3)	291 (3)	4.92
C1	2110 (4)	711 (4)	877 (4)	4.30
C2	−1729 (4)	−212 (4)	−1783 (3)	5.10
C3	586 (4)	−332 (4)	1982 (3)	4.42
C4	216 (5)	−846 (4)	3012 (3)	6.11
C5	−3303 (4)	−1381 (4)	−766 (4)	5.67
C6	538 (4)	−2854 (4)	428 (3)	4.06
C7	1940 (4)	−2256 (4)	−770 (3)	5.29
C8	2475 (4)	−3455 (4)	−310 (4)	5.80
C9	1287 (5)	−2606 (5)	−1658 (3)	7.23
C10	2791 (4)	−1259 (4)	−1142 (3)	5.11
C11	3094 (5)	−4429 (4)	−828 (4)	7.71
C12	3402 (5)	−3118 (6)	419 (4)	9.24
C13	−580 (4)	−3057 (4)	1097 (3)	5.76
Ni2	5000 (0)	5000 (0)	5000 (0)	3.41
O4	4621 (2)	3938 (2)	6259 (2)	3.97
O5	5916 (2)	3486 (2)	4508 (2)	4.23
O6	332 (3)	3537 (3)	5084 (2)	7.22
N3	3262 (3)	4521 (3)	4562 (2)	3.72
N4	1389 (3)	3816 (3)	4685 (3)	5.10
C14	6012 (4)	2431 (4)	4948 (3)	4.74
C15	4476 (4)	7989 (4)	4145 (3)	5.46
C16	4863 (4)	2801 (4)	6429 (3)	4.25
C17	4366 (5)	2241 (4)	7420 (3)	6.19
C18	6771 (5)	1500 (4)	4380 (4)	7.33
C19	2272 (4)	4355 (4)	5112 (3)	4.25
C20	2978 (4)	4293 (4)	3581 (3)	4.62
C21	1948 (4)	3379 (4)	3793 (3)	5.24
C22	4095 (4)	3845 (5)	2977 (3)	5.91
C23	2456 (4)	5565 (4)	3114 (3)	5.74
C24	1008 (4)	3437 (5)	3079 (3)	6.63
C25	2458 (5)	2037 (4)	4046 (4)	7.48
C26	1940 (4)	4682 (5)	6089 (3)	5.76
F1	−347 (40)	−1824 (33)	3081 (9)	12.84
F2	−385 (41)	−36 (21)	3426 (14)	15.37
F3	1167 (10)	−1158 (34)	3503 (9)	9.28
F4	3034 (7)	2569 (5)	772 (12)	6.89
F5	3976 (10)	1196 (14)	−5 (9)	7.02
F6	3966 (10)	1112 (12)	1480 (9)	8.08
F7	3275 (14)	1897 (25)	7393 (9)	10.24
F8	5015 (21)	1319 (20)	7786 (10)	9.47
F9	4302 (25)	3043 (11)	8018 (7)	8.57
F10	6849 (21)	392 (10)	4803 (11)	10.77
F11	6389 (15)	1440 (12)	3571 (7)	8.40
F12	7928 (9)	1961 (13)	4154 (13)	10.21
F13	498 (43)	−197 (35)	3631 (7)	12.75
F14	−978 (10)	−911 (34)	3201 (8)	9.64
F15	667 (41)	−1931 (20)	3155 (17)	14.96
F16	3340 (24)	2307 (36)	93 (18)	16.15
F17	4189 (12)	626 (13)	468 (29)	14.97
F18	3718 (26)	1663 (39)	1466 (16)	16.83
F19	5173 (27)	2278 (43)	7984 (10)	15.63
F20	4131 (41)	1104 (17)	7469 (9)	12.97
F21	3369 (27)	2820 (25)	7744 (16)	15.22
F22	6078 (20)	737 (31)	4126 (37)	22.15
F23	7500 (31)	826 (34)	4848 (17)	17.37
F24	7283 (44)	1877 (13)	3693 (18)	22.09

[a] Defined as $(4/3)a^2B(1,1) + b^2B(2,2) + c^2(B(3,3) + ab(\cos\gamma)B(1,2) + ac(\cos\beta)B(1,3) + bc(\cos\alpha)B(2,3)$.

and, with the increase of the χT product, must be related to ferromagnetic couplings. On the other hand, the decrease at low temperature is the signature of antiferromagnetic interactions. A four-spin model, suggested by the structural results and identical to that used for interpreting the magnetic data of the copper analogue, leads[31] to a rather strong intramolecular ferromagnetic coupling of 94 (8) cm^{-1} and a weak intermolecular interaction (−2.3 (1) cm^{-1}).

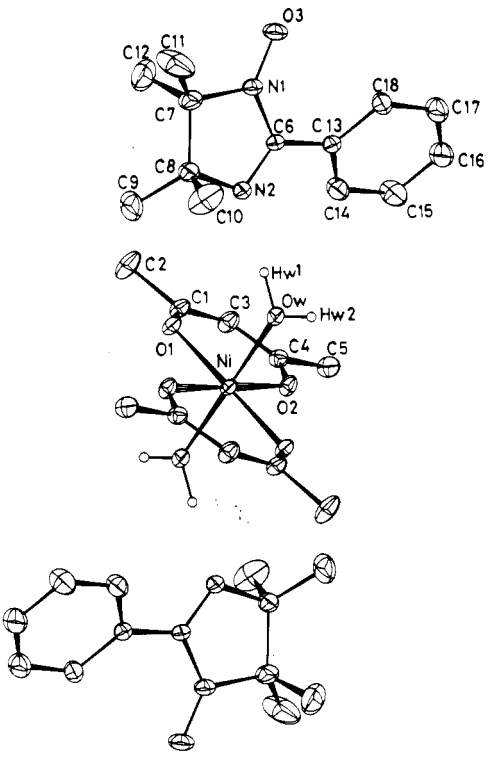

Figure 2. View of Ni(hfac)$_2$(H$_2$O)$_2$(IMPh)$_2$ (1). Thermal ellipsoids are drawn at the 30% probability level.

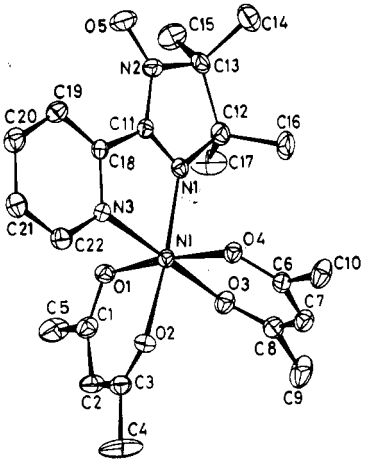

Figure 3. View of Ni(hfac)$_2$IM2-Py (2). Thermal ellipsoids are drawn at the 30% probability level.

The magnetic data of the third complex exhibit almost the same temperature dependence as **2** except that the increase of χT on lowering the temperature is more pronounced. Also, the room-temperature value (2.44 emu·K, 4.42 μ_B) is much higher than expected, pointing to predominant ferromagnetic interactions. The assumption of an isotropic contribution of the nickel ion was made, and the data were fitted to a three-spin model. However, since the structural results show short intermolecular contacts which are probably responsible for the decrease of the χT product at low temperature, a molecular field approximation[32] was included. This model affords a nitroxide–nickel ferromagnetic interaction of 59 (5) cm^{-1}. Since the asymmetric unit contains two different molecules, this coupling constant is the average of the actual interactions in the two fragments.

(31) Belorizky, E.; Friess, P. H.; Gojon, E.; Latour, J.-M. *Mol. Phys.* **1987**, *61*, 661–666.

(32) Hatfield, W. E.; Weller, R. R.; Hall, J. W. *Inorg. Chem.* **1980**, *19*, 3825–3828.

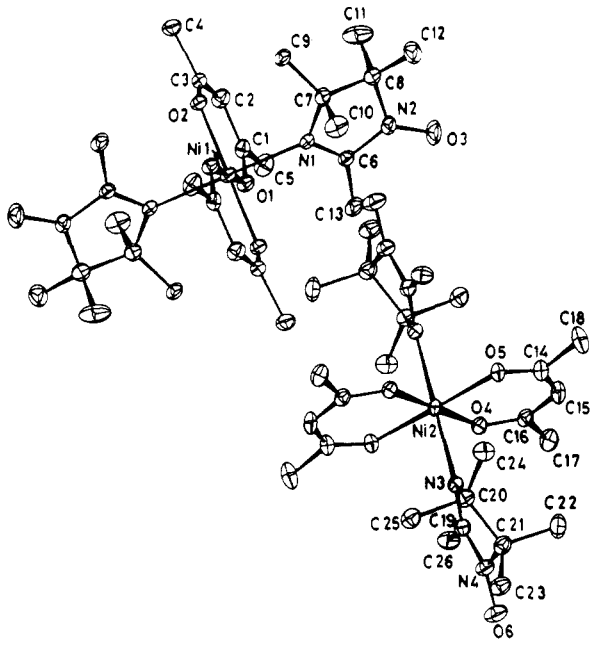

Figure 4. View of $Ni(hfac)_2(IMMe)_2$ (**3**). Thermal ellipsoids are drawn at the 30% probability level.

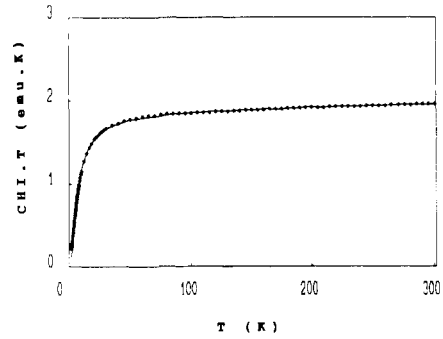

Figure 5. Temperature dependence of χT for $Ni(hfac)_2(H_2O)_2(IMPh)_2$ (**1**). The solid curve was calculated with the first set of parameters reported in Table VI.

We have studied the above systems in more detail using models which include the g factors of the different fragments (Ni(II) and nitroxide) and developing analytic expressions of the susceptibility which take into account the g factors of all the energy levels. For three-spin systems **1** and **3**, taking the Hamiltonian as $H = -2J\vec{S}_0(\vec{s}_1 + \vec{s}_2)$, where $\vec{S}_0$ and $\vec{s}_i$ stand for the spins of Ni(II) and the nitroxides respectively, the expressions for the susceptibility are as follows: For **1**

$$\chi = (3x/4kT)(((g_0/2 + 1)^2(1 + 5x^2) + g_0^2x)/(1 + 3x + 3x^2 + 5x^3)) + \mathrm{TIP}$$

where $x = \exp(2J/kT)$ and g_0 is the g factor for the Ni(II) ion; the g factor of the nitroxide ligands has been set at 2.00. For **3**

$$\chi = (3/4kT)(((g_0/2 + 1)^2(5 + x^2) + g_0^2x)/(1 + 3x + 3x^2 + x^3)) + \mathrm{TIP}$$

where $x = \exp(-2J/kT)$.

For compound **2**, which must be considered as a four-spin system, such calculations were not possible. Therefore, taking into account only the high-temperature data, a pair model described by the Hamiltonian $H = -2J\vec{S}_0\vec{s}_1$ was considered. The corresponding susceptibility was given by

$$\chi = (1/24T)((10(g_0 + 1)^2 + (2g_0 - 1)^2x)/(2 + x)) + \mathrm{TIP}$$

where $x = \exp(-3J/kT)$.

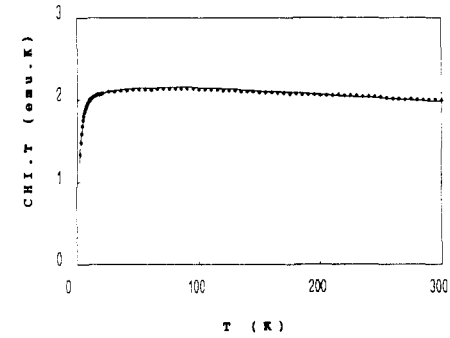

Figure 6. Temperature dependence of χT for $Ni(hfac)_2IM2\text{-}Py$ (**2**). The solid curve was calculated with the first set of parameters reported in Table VI.

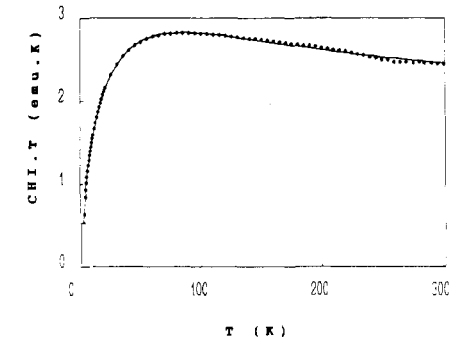

Figure 7. Temperature dependence of χT for $Ni(hfac)_2(IMMe)_2$ (**3**). The solid curve was calculated with the first set of parameters reported in Table VI.

Note that the reasonable following simplification was made: In three-spin systems, only the nickel(II)–nitroxide interaction has been considered because the first fitting scheme which involved only an average g value showed that the results were independent of the inter-nitroxide coupling constant.

The best fit values obtained using these expressions are reported in Table VI. One can note that very similar exchange parameters are obtained using both methods. However, significant differences are observed for the g and the TIP values. Although marginal interest is usually devoted to TIP values because they include most experimental defects, values of (200–300) $\times 10^{-6}$ emu obtained in the second set of parameters are in better agreement with those expected for Ni(II) ions.[33] Moreover, since the g_0's correspond to the free metal ion, a correspondence between the g_0 and TIP parameters can be made. Indeed, the Ni(II) ion in cubic symmetry has an A_2g orbital singlet ground state only coupled to a T_2g excited triplet. In the pure ionic limit, $g_0 = 2 - 8\lambda/\Delta$ and $\mathrm{TIP} = 9k/\Delta$. Taking $\lambda = 320\ \mathrm{cm}^{-1}$,[34] the experimental g_0 and TIP values lead to Δ energy gaps in the 15 000–20 000-cm^{-1} range. In fact, the consideration of covalent effects, neglected in this study, would decrease the matrix elements of the orbital moment leading to lower Δ values closer to the 10 000–15 000-cm^{-1} range and in better agreement with literature reports.

Owing to the close octahedral symmetry observed in these compounds, zero field splitting effects are expected to be weak (<1 cm^{-1}); however, their neglecting gives less meaning to the values of the intra- (J_i) as well as intermolecular (J_e) weak antiferromagnetic interactions which show up at low temperature. On the other hand, in **2** and **3**, it can be confidently stated that the intramolecular (J_i) Ni(II)–nitroxide coupling is ferromagnetic in nature and fairly large. Further support to this statement comes from the field dependence of the magnetization, shown in Figure 8for compound **2**, which is exactly that of a $S = {}^3/_2$ spin.

(33) Boudreaux, E. A.; Mulay, L. N. *Theory and Applications of Molecular Paramagnetism*; John Wiley & Sons: New York, 1976; p 126.
(34) Abragam, A.; Bleaney, B. *Electron Paramagnetic Resonance of Transition Ions*; Clarendon Press: Oxford, England, 1970; p 399.

Table V. Selected Bond Lengths (Å) and Angles (deg)

			$Ni(hfac)_2(H_2O)_2(IMPh)_2$ (**1**)				
Ni–O1	2.018 (2)	Ni–O2	2.023 (2)	Ni–Ow	2.042 (3)	Ow–Hw1	1.07 (6)
Ow–Hw2	0.752 (51)	N2–Hw1	1.71 (6)	O3–N1	1.267 (4)	N1–C6	1.391 (4)
N2–C6	1.281 (5)						
O1–Ni–O2	88.8 (1)	O1–Ni–Ow	92.0 (1)	O2–Ni–Ow	91.6 (1)		
Ni–Ow–Hw1	125 (4)	Ni–Ow–Hw2	120 (4)	Ow–Hw1–N2	175 (7)		
Hw1–N2–C6	130 (2)	Hw1–N2–C8	116 (3)	C6–N2–C8	109.7 (3)		
			$Ni(hfac)_2$IM2-Py (**2**)				
Ni–O1	2.047 (4)	Ni–O2	2.040 (4)	Ni–O3	2.022 (5)	Ni–O4	2.051 (4)
Ni–N1	2.050 (5)	Ni–N3	2.074 (5)	O5–N2	1.276 (10)	N1–C11	1.279 (9)
N2–C11	1.359 (8)						
O1–Ni–O4	173.0 (2)	O2–Ni–N1	171.5 (2)	O2–Ni–N3	175.8 (2)		
O1–Ni–O2	89.6 (2)	O1–Ni–O3	85.4 (2)	O1–Ni–N1	92.1 (2)		
O1–Ni–N3	90.5 (2)	O2–Ni–O3	88.2 (2)	O2–Ni–O4	86.8 (2)		
O2–Ni–N3	92.8 (2)	O3–Ni–O4	88.5 (2)	O3–Ni–N1	100.3 (2)		
O4–Ni–N1	92.3 (2)	O4–Ni–N3	95.7 (2)	N1–Ni–N3	78.9 (2)		
Ni–N1–C11	113.8 (4)	Ni–N1–C12	136.5 (5)	C11–N1–C12	109.7 (6)		
Ni–N3–C18	115.6 (4)	Ni–N3–C22	126.4 (5)	C18–N3–C22	117.9 (6)		
			$Ni(hfac)_2(IMMe)_2$ (**3**)				
			Molecule A				
Ni1–O1	2.021 (2)	Ni1–O2	2.028 (2)	Ni1–N1	2.202 (2)	O3–N2	1.266 (4)
N1–C6	1.288 (5)	N2–C6	1.394 (6)				
O1–Ni1–O2	91.4 (1)	O1–Ni1–N1	92.7 (1)	O2–Ni1–N1	87.3 (1)		
Ni1–N1–C6	125.2 (3)	Ni1–N1–C7	128.1 (2)	C6–N1–C7	106.6 (3)		
			Molecule B				
Ni2–O4	2.040 (2)	Ni2–O5	2.035 (2)	Ni2–N3	2.172 (3)	O6–N4	1.274 (4)
N3–C19	1.281 (5)	N4–C19	1.392 (6)				
O4–Ni2–O5	88.1 (1)	O4–Ni2–N3	88.7 (1)	O5–Ni2–N3	91.8 (1)		
Ni2–N3–C19	124.9 (3)	Ni2–N3–C20	128.1 (2)	C19–N3–C20	107.0 (3)		

Table VI. Fitting Parameters for the Magnetic Data[a]

compd	g	g_0	J_i	J_e	TIP ($\times 10^6$)	R ($\times 10^4$)[c]
1	2.084 (8)		−2.4 (1)		122 (20)	1.2
		2.147 (5)	−2.3 (1)		319 (45)	1.6
2	2.149 (8)		+94 (8)	−2.3 (2)	126 (33)	1.1
		2.182 (16)	+95 (4)		249 (52)	0.06
3	2.124 (4)		+59 (5)	−2.0 (1)[b]	93 (24)	0.6
		2.178 (8)	+57 (6)	−2.3 (2)[b]	245 (47)	0.7

[a] For each compound two sets of parameters corresponding to different treatments are reported (see text). J_i and J_e are intra- and intermolecular interactions, respectively. The Hamiltonian is defined as $H = -2J\tilde{S}_1\tilde{S}_2$; exchange parameters are in cm^{-1}. [b] zJ' as defined in ref 32. [c] $R = (\sum(\chi^{obsd} - \chi^{calcd})^2/\sum(\chi^{obsd})^2$.

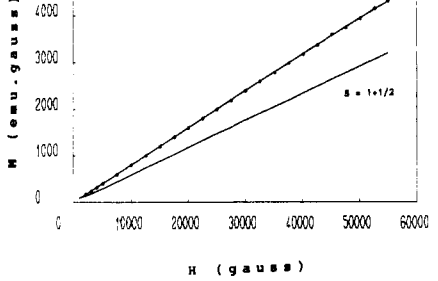

Figure 8. Field dependence of the magnetization for $Ni(hfac)_2$IM2-Py (**2**) at 25 K. The solid curves are calculated for $S = {}^3/_2$ and $S = 1 + {}^1/_2$.

Discussion

As expected, two of the adducts are N-bonded species. On the other hand, the IMPh derivative is a solvate in which the nitroxide ligands are linked through hydrogen bonds to the aquo metal fragment. Several different preparations were attempted in order to obtain the metal-bound species without success.

Our present knowledge of the coordination chemistry of the imino nitroxides does not afford a straightforward answer to these observations, but qualitative understanding may be drawn out from steric and electronic considerations. It is obvious that, in imino nitroxides, the imino nitrogen coordination site is sterically crowded by the *α-gem*-dimethyl group because binding to a metal ion is likely to bring one of these methyl groups in close contact with another ligand. Nevertheless, IMMe, in giving the N-bonded derivative shows that the Ni coordination sphere is open enough to accommodate this ligand. In the case of IMPh, the presence of the sterically demanding phenyl group probably increases the crowding so much that this ligand is not bound. It can be also noted that the phenyl group has electron-withdrawing properties which lessen the base strength of the ligand to some extent compared to the methyl-substituted analogue. On the other hand, the binding of IM2-Py, in which the pyridyl group has as much steric requirement as a phenyl group, is ensured for two reasons. In addition to the chelate effect which is probably a significant driving force, the bidentate character of this ligand allows fulfillment of the octahedral preference of the Ni(II) ion in a monoadduct. This preference would require two IMPh ligands to be metal bound, leading to an unrealistic steric crowding of the metal coordination sphere.

Another important structural feature of the adducts described in this work is the absence of extended species such as those obtained with the nitronyl nitroxide analogues.[2i,35] This happens in imino nitroxide derivatives because the two coordination sites (N and O) are very close (≃3.5 Å to be compared to the O–O distance, 4.8 Å, in nitronyl nitroxides). Thus, when two metal ions are bridged, this proximity makes more probable steric interactions between groups supported by adjacent metal centers. Accordingly, it is sterically difficult for an imino nitroxide to bridge two octahedral metal centers such as Ni(II). These results

(35) Caneschi, A.; Gatteschi, D.; Renard, J.-P.; Rey, P.; Sessoli, R. *Inorg. Chem.* **1989**, *28*, 2940–2944.

are strongly supported by the structural characteristics of related copper(II) complexes.[16] Surprisingly, IMPh bridges $Cu(hfac)_2$ fragments in a trinuclear adduct where the N(nitroxide)–metal bond lengths are shorter than in nickel(II) compounds. Such a polynuclear complex was obtained because, in being only five-coordinated, the N-bonded copper ions can release steric constraints. Thus, this propensity of Cu(II) for being only five-coordinated allows the coordination of sterically crowded ligands and, also, is the cause for the reported bridged structures which are never observed for the Ni(II) analogues. Also interesting is the comparison of the imino nitroxide fragments in $(Cu(hfac)_2)_3(IMPh)_2$, where the interaction between the N-bound copper ion and the ligand is strongly ferromagnetic, and in **1**, where the same ligand is very weakly coupled to the metal through hydrogen bonding. It can be seen that, within experimental error, these two fragments are identical. In contrast to strongly interacting metal–nitronyl nitroxide adducts where a substantial lengthening of the NO bond is observed, it seems that the N-coordination of an imino nitroxide is not reflected in structural modification.

Since in compound **1** the free radical is not directly bound to the Ni(II) ion and each molecular unit is well shielded from neighbors, its antiferromagnetic behavior has been considered as arising from exchange interaction through the water molecule. To the best of our knowledge, this is the first determination of a nitroxide–metal interaction mediated by hydrogen bonding. The magnitude of this interaction (-2.4 (1) cm^{-1}) is in agreement with the weakness of such a bond. On the other hand, the two other complexes have contrastingly different magnetic properties because the nitroxide ligands are metal bound. Although the ground state reflects antiferromagnetic intermolecular interactions, the intramolecular coupling is, in both compounds, ferromagnetic in nature and fairly large. Compared to the nitronyl nitroxides, the binding of an imino nitroxide to a Ni(II) ion through the imino nitrogen leads to exchange interactions of the same order of magnitude but of reverse sign. The same situation was reported for copper derivatives of the same ligands,[16] in which large ferromagnetic metal–ligand interactions were observed. Understanding of the magnetic properties of both classes of complexes relies on the same molecular orbital considerations: in Cu(II) compounds, the binding of the nitroxide through the imino nitrogen occurs in such a way that, in the reported examples in which the metal magnetic orbital has d_{z^2} or $d_{x^2-y^2}$ symmetry, the ligand and metal magnetic orbitals are orthogonal.[16] In the Ni(II) adducts, whatever the axial or equatorial coordination of the ligand, the geometric parameters of the binding are identical to those observed in the copper species. Therefore, the same symmetry considerations apply to these compounds and the observed ferromagnetic behavior also is the consequence of magnetic orbital orthogonality.

Owing to antiferromagnetic intermolecular interactions, these complexes have a low-spin ground state. This behavior results from contacts between uncoordinated NO groups related by cell translations or a center of symmetry. In such an arrangement, the extent of the coupling of the two NO groups depends on their distance and on the orientation of the π^* orbitals. In **2** and **3**, these orbitals are not favorably oriented for strong overlap because, in both compounds, the shortest inter-NO distance is larger than 3.57 Å and the angle between the plane defined by the two NO groups and the plane of the π system of the nitroxides is larger than 118°. Although the interpretation of the data did not take into account zero field splitting effects, the values reported in Table VI are consistent with a reported semiquantitative theoretical study.[36]

Except for a manganese derivative,[37] all metal complexes of imino nitroxides described so far exhibit ferromagnetic exchange couplings. In this respect, they are very different from the extensively studied nitronyl nitroxides derivatives in which antiferromagnetic interactions are the rule. The coordination chemistry of both classes of free radicals also is very different. As a consequence of their bridging properties, nitronyl nitroxides afforded interesting chain compounds while for imino nitroxides such extended species seem to be difficult to design using metal hexafluoroacetylacetonates. However, the presence of the imino nitrogen site which has strong donor properties will allow the design of metal complexes derived from less acidic and less crowded metal centers. This possibility associated with the ferromagnetic character of the metal-nitroxide interaction is promising for further development in the synthesis of high-spin molecular species.

Supplementary Material Available: Tables giving a crystal data summary (Table SI), bond lengths and angles (Tables SII–SVII), and anisotropic thermal parameters (Tables SVIII–SX) (17 pages). Ordering information is given on any current masthead page.

(36) Caneschi, A.; Ferraro, F.; Gatteschi, D.; Rey, P.; Sessoli, R. *Inorg. Chem.* **1990**, *29*, 1756–1760.

(37) Rey, P.; Luneau, D.; Cogne, A. *Magnetic Molecular Materials*; Gatteschi, D., Kahn, O., Miller, J. S., Palacio, F., Eds.; Nato Asi Series; Kluwer: Dordrecht, The Netherlands, 1991; Vol. 198, pp 203–214.